# seaDecadal trends in phytoplankton production in the Pacific Arctic Region from 1950 to 2012

Victoria Hill[1]*; Mathieu Ardyna[2]; Sang H Lee[3]; Diana E. Varela[4]

* Corresponding author

[1]Department of Ocean, Earth, and Atmospheric Sciences; Old Dominion University; Norfolk, VA. USA.

[2]Sorbonne Universités, UPMC Univ Paris 06, INSU-CNRS, Laboratoire d'Océanographie de Villefranche, 181 Chemin du Lazaret, 06230 Villefranche-sur-mer, France

[3]Department of Oceanography, Pusan National University; Busan 609-735, Korea

[4]Department of Biology and School of Earth and Ocean Sciences; University of Victoria, P.O. Box 1700, Station CSC, Victoria, B.C. V8W 2Y2, Canada

To be submitted to Deep Sea Research II – Topical Studies in Oceanography.

Keywords: Polar Waters; Primary Production; Climate Changes; *In situ* measurements

**Abstract**

This paper provides a synthesis of available *in situ* primary production (PP) measurements from the Pacific Arctic Region (PAR), collected between 1950 and 2012. Seasonal integrated primary production (IPP) across the PAR was calculated from 524 profiles, 340 of which were also analyzed to determine the average vertical distribution of PP rates for spring, summer and fall months. The Chirikov Basin and Chukchi Shelf were the most productive areas, with the East Siberian Sea, Chukchi Plateau and Canada Basin the lowest. Decadal-scale changes were indicated in the southern Chukchi Sea, and across Hanna Shoal. In the southern Chukchi Sea in August, IPP increased significantly from 113 ±35 mg C $m^{-2}$ $d^{-1}$ in 1959 and 1960 to 833 ±307 mg C $m^{-2}$ $d^{-1}$ in the 2000s. Increases in the magnitude of IPP were accompanied by variations in the vertical distribution, the subsurface peak observed in the 1959/60 was not present in the 2000s. The mechanism behind this change was undetermined but could have included changes in stratification, mixing or surface distribution of water masses as well as methodological differences. Over Hanna Shoal, the phytoplankton surface bloom now occurs earlier by several weeks compared to 1993, linked to increases in light due to earlier sea- ice retreat. In 1993 with sea ice still present in the region the surface bloom occurred in August, in 2002 and 2004 this same period was characterized by open water and low surface PP and strong subsurface production. This dataset provides a region-wide quantification of IPP and decadal trends and highlights the need for a cooperative monitoring program to observe the long-term impacts of climate change in the Arctic ecosystem.

## 1.0 Introduction

The Pacific Arctic Region (PAR) encompasses areas influenced by Pacific water inflow into the Arctic. The flow of heat, freshwater, and nutrients introduced by Pacific water is a primary driver of both the physical and biological state in the Bering Sea, the Chukchi Sea, the western portion of the Beaufort Sea, the East Siberian Sea and the Canada Basin. The PAR has traditionally contained a highly seasonal and productive ecosystem which supports a diverse and high biomass benthic community (Grebmeier et al., 1988; Hill and Cota, 2005; Mathis et al., 2014).

Two areas with some of the highest integrated primary production (IPP) within the Arctic Ocean are included in the PAR, the northern Bering Sea area referred to as the Chirikov Basin, and the Chukchi Sea (Fig. 1). Both *in situ* and satellite observations in the Chirikov Basin have estimated IPP to range from ~80 g C $m^{-2}$ $yr^{-1}$ on the interior shelf to up to 480 g C $m^{-2}$ $yr^{-1}$ in the Anadyr water plume (Springer and McRoy, 1993; Springer et al., 1996 and references therein; Hill et al., 2013; Brown et al., 2011). The Chukchi Sea has long been an area of high productivity with annual IPP ranges between 170 and 720 g C $m^{-2}$ $yr^{-1}$ across the shelf (Sakshaug et al., 2004; Arrigo et al., 2008; Hill et al., 2013; Varela et al., 2013). In contrast, the Eastern Siberian Sea and Canada Basin are low productivity areas. Phytoplankton growth in open water in the Canada Basin can reach highs of ~100 mg C $m^{-2}$ $d^{-1}$ for the July to September growing season (Lee and Whitledge, 2005; Varela et al., 2013). However, on average rates are lower at 48 mg C $m^{-2}$ $d^{-1}$ in the Canada Basin (Varela et al., 2013) and 8 to 29 g C $m^{-2}$ $yr^{-1}$ in the East Siberian Sea (Codispoti et al., 2013; Slagstad et al., 2011). Due to chronic undersampling in the basin, annual rates should be taken with caution, but have been estimated at 2.5 to 21 g C $m^{-2}$ (Lee et al., 2010). The Beaufort shelf (Fig. 1) while not as productive as the Chukchi Sea can have high growth rates associated with the ice edge, reaching 200 mg C $m^{-2}$ $d^{-1}$ (Carmack et al., 2004; Mundy et al., 2009).

One characteristic ubiquitous across the PAR in summer is a subsurface primary production maximum (SPM) (Arrigo et al., 2011; Ardyna et al., 2013; Hill and Cota, 2005; Hill et al., 2013; Martin et al., 2010; McLaughlin and Carmack, 2010; Martini et al., 2016). This feature forms after the surface phytoplankton bloom declines due to nutrient limitation, induced by stratification of the water column. An SPM forms at the nutracline, where light availability is still adequate to stimulate primary production (PP). In a modeling exercise, Popova et al. (2010)

53 estimated that the SPM accounts for 46% of annual Arctic Ocean production. Hill et al., (2013)
54 concluded that 70% of Arctic IPP in the summer (July to September) occurred in the SPM, and
55 Martin et al., (2013) observed 65 to 90% of annual IPP in the Beaufort Sea occurring at the SPM,
56 driven by stratification and surface oligotrophic conditions.
57 The PAR has experienced a dramatic change in seasonal ice retreat and subsequent thinning
58 of the ice pack. In the Chukchi Sea, ice survival has declined by 30 d $dec^{-1}$ between 1979 and
59 2008 (Frey et al., 2014), due to a combination of earlier melt and later freeze-up (Stroeve et al.,
60 2014). Ice breakup now starts in April in the southern Chukchi and in June along the Chukchi
61 Sea shelf break (Frey et al., 2015). In the Beaufort Sea, a 1.24 d $yr^{-1}$ decline in the presence of
62 sea ice between 1970 and 2012 has accelerated to 12.84 d $yr^{-1}$ over the 2000 to 2012 period (Frey
63 et al., 2015). There is also a general thinning of the Arctic ice pack, which goes in hand with
64 losing much of the multiyear ice. The overall mean ice thickness for the Arctic has decreased
65 from 3.64 m in 1980 to 1.89 m in 2008 (Kwok and Rothrock, 2009). The thickness of the ice
66 pack has undergone the greatest change in September, with a thinning equivalent to 51 cm $dec^{-1}$
67 in the Chukchi Sea, leading to current projections that the PAR is moving towards an entirely
68 first-year ice pack (Frey et al., 2014). Linked with changes in the ice pack are summertime
69 warming anomalies as high as 2.5 °C, due to radiative heating in ice-free water (Steele et al.,
70 2008; Timmermans and Proshutinsky, 2015). The loss of sea ice has resulted in an Arctic-wide
71 increase in primary production estimated from satellite retrievals, equivalent to 27.5 Tg C $yr^{-1}$
72 since 2003. Much of this has been associated with increased ice retreat in the Chukchi and
73 Siberian Seas (Arrigo et al., 2008). A recent study indicated that Arctic NPP increases reached a
74 plateau in 2011 (Kahru et al., 2016), suggesting that the region may have reached its maximum
75 supportable phytoplankton growth.
76 Ultimately the impact of changes in the physical and chemical properties of the PAR are yet
77 to be determined, but will likely include modifications in plankton phenology and carbon
78 cycling, linked to shifts in the water temperature, timing, and length of growth seasons. Recent
79 observations of high under-ice phytoplankton accumulations within ~100 km of the ice edge may
80 be an indication of a changing IPP regime, in which water column phytoplankton growth can be
81 initiated and sustained under the ice due to increased light transmission (Perovich et al., 2008;
82 Arrigo et al., 2012; Churnside and Marchbanks, 2015). If the spring bloom now occurs earlier
83 than historically observed, then the net result of an Arctic-wide shift from multiyear to seasonal

ice could be a permanent change in the timing of the pelagic bloom, with consequences for secondary producers and higher trophic levels. For example, for copepod offspring to survive, copepod reproduction has to match the timing of the ice algal bloom, and copepodite growth has to match the timing of the following pelagic bloom (Soreide et al., 2010; Leu et al., 2011). When the pelagic bloom is shifted earlier due to increased light availability, resulting copepod biomass can decrease dramatically (Soreide et al., 2010; Leu et al., 2011). Reduced or lack of zooplankton grazing under these conditions would lead to greater settling of algal carbon to the seafloor benefiting benthic consumers. It is critical, therefore, in this time of environmental variability, to quantify water column IPP, and identify changing patterns in distribution, timing, and magnitude.

By delineating the PAR into regions (Chirikov Basin, southern and northern Chukchi, Beaufort, East Siberian Seas, Chukchi Plateau and Canada Basin), we reveal here a diversity of productive regimes and specificities in their seasonal vertical PP distribution. By combining published data sets for this region, our goal was to detect potential decadal trends in both vertical PP profiles and seasonal IPP.

## 2.0 Methods

Using the delineation from Hill et al., (2013) PP data were analyzed for the following regions: Chirikov Basin, southern Chukchi, northern Chukchi (inflow shelves), Beaufort Shelf, East Siberian Seas (interior shelves), the Chukchi Plateau and Canada Basin (Basin) (Fig. 1).

The *in situ* PP data were obtained from the ARCSS-PP database 1950 to 2007 (Matrai et al., 2013; Arctic System Science Primary Production; http://www.nodc.noaa.gov/cgi-bin/OAS/prd/accession/details/63065) and individual PIs associated with cruises since 2003 (Table 1). Matrai et al. (2013) described the spatiotemporal heterogeneity of the ARCSS-PP dataset. Caution is recommended in the analysis of datasets such as these due to inherent and potential biases. This combined dataset contains 524 vertical profiles of PP measurements (Table 1). The data were collected by numerous investigators employing many methods and analytical protocols and represent individual, national and international research efforts. We restricted our use of the data to (i) net phytoplankton primary production, (ii) incubations longer than 12 hours and (iii) profiles with a minimum of three depth measurements. IPP was calculated for each profile by a trapezoidal integration from the uppermost data point in the water column to the

deepest point. The mean IPP for each region and month was calculated using all 524 available profiles.

Not all data points included the associated sample and incubation light levels, so a subset of 340 stations for which a light level was reported were used to determine mean profiles of PP for all regions. Mean profiles based on geometric depth were calculated for the southern Chukchi Sea for August during the periods 1959 and 1960, and 2004 to 2007 to facilitate decadal comparisons. For both analyses all profiles were normalized to the maximum PP within each profile so that the maximum PP was set to the value of 1 and all other measurements in the profile were relative to that maximum. The mean normalized profile for each region was then calculated.

The data was separated into four time periods to facilitate analysis: (i) May and June, designated as spring; (ii) July, early summer; (iii) August, late summer; and (iv) September and October, fall.

Rasterization of point measurements was achieved in ArcMap software version 10.2.2 by generating a delaunay triangular network and interpolating to a raster using the Geoprocessing toolbox with an inverse distance weighted interpolation.

Sea-ice concentration maps were downloaded from the Nimbus-7 SMMR and DMSP SSM/I-SSMIS Passive Microwave Dataset at the National Snow and Ice Data Center (Cavalieri et al., 1996 updated yearly) as GeoTIFFs and mapped using ArcMap software version 10.2.2.

All data are presented as arithmetic means ±1 standard error. The overall statistical significance of means was determined by 1-way ANOVA, followed by Tukey's significant difference criterion for individual comparisons when ANOVA returned statistically significant results. All statistical analysis were conducted using the Matlab2015b © statistical toolbox.

## 3.0 Results

### *3.1 Spatial and temporal distribution of in situ data.*

A total of 524 vertical profiles of PP measurements were available from our combined database (Table 1). Distribution of these stations was not uniform in time or space with 70% of the profiles collected during summer months (July and August; Fig. 2A through D). For stations occupied in the spring (May and June), 80% of measurements were collected after 2000 and are distributed from the Chirikov Basin to the Chukchi shelf break, following the western coast of

Alaska (Fig. 2A). Measurements made in July were confined to areas south of Point Hope (68.35, -166.76) before 1990, and have extended north of Point Hope since 2000 into the Beaufort shelf, East Siberian Sea and Canada Basin (Fig. 2B). In August measurements collected before 1990 were confined to the area south of Icy Cape (70.33, -161.87; Fig. 2C), but in the decades since 1990 measurements extended across the northern Chukchi shelf, onto the East Siberian Sea and well out over the Chukchi Plateau and Canada Basin. During the fall (September and October) measurements are sparse and predominately collected after 2000, with profiles available in the Beaufort shelf, East Siberian Sea, Chukchi shelf and Chukchi plateau (Fig. 2D).

*3.2 Vertical profiles of primary production based on light levels.*

*3.2.1 Inflow shelves*

In the Chirikov Basin (north Bering Sea), spring PP was highest between the 50 and 10% light level (LL; Fig. 3A). This SPM became more prominent in July, with a defined peak around the 30% LL. On average ~50% of all water column PP during these periods occurred between the 50 and 10% LL (Table 2). Later in the growth season (August, September and October) the SPM was eroded with rates increasing only slightly between the surface and the 50% LL, and then decreasing with decreasing light intensity (Fig. 3A). This late summer to fall loss of the previously prominent SPM is apparent in the shift towards ~60% of PP occurring above the 50% LL (Table 2).

On the southern Chukchi shelf, an SPM was present in both the spring (May and June) and early summer July (Fig. 3B) and was predominately present on the east side of the Chukchi shelf. The SPM localized ~50% of PP below the 50% LL (Table 2). During the late summer (August), and fall (September and October) PP was highest at the surface (Fig. 3B), with ~66% and 60% respectively of all PP taking place above the 50% LL (Table 2).

On the northern Chukchi shelf, a strong SPM was observed in both the spring and early summer (Fig. 3C), with the SPM in July occurring deeper at the 10 to 5% LL compared to 30% LL in the spring. This results in over 70% of all PP during July occurring below the 50% LL (Table 2), and 25% of PP in some stations occurring at light levels below 10%. During August there was high variability in observed profiles with no consistently defined peak, producing a

relatively homogenous distribution from the surface to the 5% LL. In the fall PP was consistently highest at the surface and decreased with decreasing light (Fig. 3C).

*3.2.2 Interior shelves*

On the Beaufort shelf, a broad subsurface peak was observed in May and June between 50 and 5% LL and was two times greater relative to surface rates (Fig. 3D). This subsurface peak accounted for 62% of water column PP during the spring (Table 2). Vertical profiles observed on the Beaufort shelf in July were highly variable with many including a SPM, leading to a mean profile that includes both surface and subsurface peaks (Fig. 3D), but that allocated ~50% of all PP below 50% LL (Table 2). During the late summer and into the fall, PP was highest at the surface and decreased with depth (Fig. 3D), distributing the majority of PP above the 50% LL (Table 2).

In the East Siberian Sea, no data was available for the spring, and only three profiles were available for July, one with a prominent SPM at 1% LL and others with highest PP at the surface. The divergence of observations for July results in an unusual mean profile, with a peak at both the surface and at the 1% LL (Fig. 3E). In August, PP was highest at the surface with ~65% of all PP occurring above the 50% LL (Fig. 3E, Table 2). In the fall a small SPM was observed between 50 and 10% LL (Fig. 3E), this is in in contrast to all the other regions for this period.

*3.2.3 Basin*

Data with reported light depths were only available in late summer and fall in the Chukchi Plateau and Canada Basin. In August, profiles were variable, and the average PP was homogenous to approximately the 5% LL (Fig. 3E). In the fall PP was consistently highest at the surface and decreased with depth. These profiles show that 50 and 60% of total PP respectively in late summer and fall occurred above the 50% LL (Table 2).

*3.3 Decadal differences in the vertical profiles of primary production*

This dataset does not afford the opportunity to look at broad scale changes in PP in the PAR over time, as samples are sparse in space and time. However, enough repeat observations are available to investigate shifts in the southern Chukchi Sea and along the Hanna Shoal transect (see Fig. 1). Overlapping measurements were available in the central channel of the southern Chukchi Sea during August for 1959 and 1960 (14 profiles) and from 2004 to 2007 (6 profiles; Fig. 4A). During 1959 and 1960, the average profile presented with a broad subsurface peak

between 10 and 40 m (Fig. 4B). In data collected between 2004 and 2007, the average profile was one with highest PP at the surface and decreasing rates with depth (Fig. 4B). The total water column IPP from the 1959 and 1960 measurements was statistically lower at 114 (±34) mg C $m^{-2}$ $d^{-1}$ compared to higher values measured in the 2004 to 2007 period of 833 (±307) mg C $m^{-2}$ $d^{-1}$ (Fig. 4C; ANOVA $p < 0.05$). The mean and standard errors for IPP collected in the 1980s and 2010s are also shown in Fig. 4C together with the 1959/1960 and 2000s measurements; however, there were only three observations in the 1980s and one in the 2010s.

The Hanna Shoal transect was occupied in August of 1993, 2002 and 2004. Measurements were collected starting on the shelf and continuing over the shelf break and into the Canada Basin (Fig. 1, Fig. 5). In 1993 ( 1 – 4 August), PP was highest in the top 20 m, with highest rates of ~30 mg C $m^{-2}$ $d^{-1}$ at stations over the shelf break (Fig. 5A). In 2002 (6 - 12 August), PP exceeded the 1993 rates with surface values of ~60 mg C $m^{-2}$ $d^{-1}$ and a strong SPM between 20 and 40 m depth that was five times that of the surface (Fig. 5B). Observations in 2004 were collected during 13 - 17 August (Fig. 5C). Surface PP rates were depressed compared to previous years at ~5 mg C $m^{-2}$ $d^{-1}$, with a well-developed SPM at around 40 m depth (~10 to 20 mg C $m^{-2}$ $d^{-1}$) that was three times that at the surface. Sea-ice cover was noticeably different between the 1993 and the 2002 and 2004 sampling periods. Between 20 to 80% ice cover was in place at the transect stations during the entire time of the 1993 occupation (Fig. 6 top). By 1 August 2002 Hanna Shoal transect was free of ice, five days before the first PP measurements. The ice did move back into the region during the measurements, but less than 10% ice cover was present on the transect (Fig. 6 middle). In 2004, the transect was covered by less than 10% ice cover at the beginning of August and was entirely ice free by the occupation of the first station on 10 August (Fig. 6 bottom).

*3.4 Integrated water column PP*

In the Chirikov Basin, IPP was highest in May, July and August (Table 3, Fig. 7), with maximum rates of 1800 (± 260) mg C $m^{-2}$ $d^{-1}$ measured in July. Variation in IPP was high across all months, and there was no statistical difference in IPP between seasons (ANOVA, $p < 0.05$). In the southern Chukchi Sea, IPP was lowest in August through the fall, with highest IPP in May and July (Table 3). However, there are only two data points in May for the southern Chukchi Sea with highly different observations resulting in a large standard error in the mean for this month.

In May, June and July, the highest IPP was observed in the central channel (Fig. 7A and B), and in the fall a hot spot was discerned on the west side of the Chukchi shelf (Fig. 7D). In the southern Chukchi Sea IPP in July was statistically higher than June, August, and September (ANOVA $p < 0.05$). In the northern Chukchi region, IPP was highest in June and July (Table 3, Fig. 7), with lowest rates observed in May and the fall. The magnitude of IPP in both June and July in the northern Chukchi were statistically higher (ANOVA $p < 0.05$) than May, August, and September (Table 3). Highest rates in the northern Chukchi Sea were consistently found along the Alaska coast in May, over Hanna Shoal in July and along the shelf break in August (Fig. 7A, B, and C). On the Beaufort shelf, the highest PP was observed close to the coast in June and July (Table 3, Fig. 7A and B) with lowest rates in August and fall (Table 3, Fig. 7C and D). Rates in the Beaufort Sea during June and July were approximately half of those observed in the Chukchi Sea during the same period. In June, IPP in the Beaufort was statistically greater than that observed in September (Table 3, ANOVA, $p < 0.05$). Data from the East Siberian Sea was sparse, and rates were depressed all year (< 132 mg C $m^{-2}$ $d^{-1}$) compared to the neighboring north Chukchi Sea (Fig. 7A through D), with no statistical difference between the months (Table 3). The lowest IPP on the Chukchi Plateau and Canada Basin, occurred in May and September (Table 3), with elevated rates during June and July (Table 3), but were not found to be statistically different from May, August, September & October. Considering all regions, IPP in PAR was highest in the Chirikov Basin during May, on the Chukchi shelf in June and July, and again in the Chirikov Basin during late summer and fall (Table 3, Fig. 7).

## 4.0 Discussion

### *4.1 Chirikov Basin*

The profiles of PP in the Chirikov Basin for May/June and July likely represent conditions after the surface bloom, with PP limited due to water column stratification that prevents vertical mixing and replenishment of nutrients (Cullen, 1982; Sharples et al., 2001). The input of fresh water from ice melt in the spring can enhance stratification and surface nutrient limitation, providing conditions for the SPM to form. The SPM observed between 50 and 15% LL in May and June indicates that the surface bloom occurred before May. Ice breakup in the area just south of the Bering Strait now occurs in mid-April (Frey et al., 2015), so the surface bloom would have taken place under the melting ice pack before wide-scale open water conditions developed.

Recent observations of under-ice phytoplankton blooms (Arrigo et al., 2012; Lowry et al., 2014), indicate that this is a reasonable assumption. The northward transport of nutrients through this area in the summer (Coachman, 1993) can support high surface productivity, leading to the shallowing of the subsurface peak through August while IPP remains high. In the fall the subsurface peak had disappeared, and PP was highest at the surface, although rates were the lowest of the year. This is typical of a fall bloom mechanism where vigorous mixing replenishes nutrients, but low light limits photosynthetic rates.

In May and June, ice breakup and retreat is well underway in the Chirikov Basin and the highest IPP was observed south of St. Lawrence Island (Figs. 1, 8), which has been linked with a well-known hot spot in benthic PP and is the location of a persistent polynya (Grebmeier et al., 1988; Stringer and Groves, 1991). Widespread open water conditions in July and August imply that IPP would no longer be light limited and instead is likely driven by the availability of nutrients. Hot spots in IPP are found closer to the Bering Strait and are associated with the high nutrient Anadyr water transiting this area (Cooper et al., 1999). In the absence of observations before May, we estimate that the surface bloom in April generated rates similar to those seen in May and June, in this case, the annual rates for the Chirikov Basin would be on average ~240 g C $m^{-2}$ $yr^{-1}$. This value is similar to the estimates of >230 g C $m^{-2}$ $yr^{-1}$ from Sakshaug et al. (2004 and references therein) and ~170 g C $m^{-2}$ $yr^{-1}$ from Ardyna et al. (2013). Annual rates from nutrient drawdown have been estimated at 100 (50 – 200) g C $m^{-2}$ $yr^{-1}$ (Codispoti 2013), although those authors highlighted that seasonal changes in water masses make it hard to estimate net community production from nutrient drawdown. This area of the Bering shelf is highly productive and contributes the highest carbon uptake in the PAR. Satellite retrievals of IPP indicate highest annual rates of ~240 g C $m^{-2}$ $yr^{-1}$ occur just to the southwest of the Bering Strait with a gradient to the south approaching 160 – 200 g C $m^{-2}$ $yr^{-1}$ at St. Lawrence Island (Brown et al., 2011) , which agrees with our observations. Despite the presence of an SPM in the Chirikov Basin, satellite estimates are effective at approximating annual rates. However, the satellite retrievals for the summer (< 1 g C $m^{-2}$ $d^{-1}$) appear to be an underestimation compared to *in situ* rates for July and August of 1.8 and 1.6 g C $m^{-2}$ $d^{-1}$ respectively (Arrigo and van Dijken, 2011). These results agree with those at a pan-Arctic scale, showing that vertical PP variations have a limited impact on annual Arctic-wide depth-integrated PP estimates (Arrigo et al., 2011). Such SPMs are, however, significant seasonal features with a substantial impact on regional

depth-integrated PP estimates, especially when surface nitrate is exhausted under highly stratified and oligotrophic conditions (Ardyna et al., 2013).

*4.2 Southern Chukchi*

The presence of an SPM at ~15% LL in the southern Chukchi in May/June suggests that a surface bloom had likely already occurred and that surface nutrient supply was depleted leading to higher growth rates at the subsurface nutricline. This feature was also described by Brown et al. (2015) and appears to be well-developed on the Chukchi shelf by the time of full ice retreat, meaning that there must be considerable surface production occurring under the melting ice pack before the formation of the SPM. Of the profiles available in this region for spring, two were collected in May and four in June, so the average profile presented here is at best a representative of June conditions, although so few data points make it difficult to establish a consensus. As this area on average experiences ice breakup from mid-May through June (Frey et al., 2015), the surface bloom is likely occurring sometime during May when the ice pack becomes fractured, and melt ponds are forming. Analysis of satellite data from 1998 to 2002 revealed that under-ice blooms are far more prevalent than previously thought, being present across the Chukchi shelf in every year of the study (Lowry et al., 2014). It is, therefore, likely that observations in this region since the late 1990s have consistently underestimated the true magnitude of the spring PP by missing the under-ice blooms. The SPM was not present in August, September, and October when integrated PP rates were low, suggesting nutrient depletion. The mixed layer depth (MLD) in the Chukchi Sea is shallowest in July and August at approximately 12 m deep (Peralta-Ferriz and Woodgate, 2015), and nutrient profiles show nitrate depletion to a depth of ~20 m for July through September (Codispoti et al., 2013). In September, reduction in light availability due to sun angle would also have contributed to depressed PP rates. Therefore, nutrient and light limitation in the MLD could account for the decreased IPP in summer and fall.

Highest PP rates for this region were consistently observed in the central part of the shelf along the dividing line between the warm Alaskan Coastal Current to the east and the colder nutrient-rich Bering shelf waters on the west (Woodgate et al., 2015). There is a lack of measurements on the western side of the shelf, but from the distribution of the high-nutrient Anadyr Water, which hugs the left side of the Chukchi shelf through the spring and summer, we would expect this area to have rates at least as high as the central channel. This is borne out in satellite estimates where IPP from the western side of the Chukchi was twice that of the eastern

side (Arrigo et al., 2008; Hill et al., 2013). PP rates were highest in July, at a time when the SPM was pronounced, and approximately one month after ice retreat. In comparison, IPP in August was ten times lower. An analysis of a year of mooring data at approximately 40 m depth in the central Chukchi shelf (68° 20.5'N, 172° 29.8'W, Fig. 4A) shows that while June and July experience some degree of warming from – 2° to 0° C, in August the water becomes fresher and warmer (rising above freezing) (Woodgate et al., 2005). Our suggestion is that during July a thermocline is present with an associated nutricline allowing for high subsurface PP rates. The loss of the SPM in August could be caused by deepening of the thermocline perhaps due to wind action which mixes phytoplankton below the euphotic zone causing the loss of the SPM and lower IPP. This could also be compounded by the increased abundance of heterotrophic Picozoa in Pacific Water, found to decrease the magnitude of the subsurface chlorophyll maximum in the Beaufort Sea (Monier et al., 2015).

The annual rate in the south Chukchi was estimated here at 208 g C $m^{-2}$ $yr^{-1}$, which makes this the second highest IPP in the PAR. Codispoti et al. (2013) estimated a rate of 36 g C $m^{-2}$ $yr^{-1}$, much lower than our rate and at the lower end of the range reported by Sakshaug et al. (2004) ranging from 20 to 400 g C $m^{-2}$ $yr^{-1}$. Arrigo et al. (2008) reported satellite retrieved rates approaching 400 g C $m^{-2}$ $yr^{-1}$ for the central channel but showed significant inter-annual variation for this region.

Due to the lack of historical *in situ* measurements in April and May, the early phytoplankton bloom if present has consistently been missed since observations began, and therefore we expect that previous research has underestimated the growth season and therefore the annual PP for this region.

*4.3 Northern Chukchi*

The northern Chukchi Sea follows a similar pattern to the southern region, in that an SPM is present in May/June suggesting that under-ice surface blooms had already occurred. This is very early considering that ice breakup does not occur until June, although the Chukchi polynya which is located along the Alaskan coastline is a persistent feature starting in March (Stringer and Groves, 1991; Frey et al., 2015). Interestingly, IPP rates in June were among the highest of the growing season for this region, indicating that strong growth is occurring while ice is still present in the area. In July, when the area experiences widespread open water conditions, a

362 strong subsurface PP peak was present at the base of the euphotic zone that can be attributed to
363 surface nutrient limitation due to strong thermohaline stratification (Codispoti et al., 2013;
364 Peralta-Ferriz and Woodgate, 2015). Areas of highest IPP were located at the shelf break, which
365 is influenced by the shelf break jet that brings nutrient-rich Bering Sea water into the area (Gong
366 and Pickart, 2015) and strong easterly winds that induce upwelling of nutrient-rich water from
367 the deep Canada Basin (Spall et al., 2014). Rates in July are as high as in June, especially in the
368 Chukchi polynya area, where open water persists since the early spring (Stringer and Groves,
369 1991). This dataset includes a data point from the 2011 ICESCAPE cruise
370 (http://ocean.stanford.edu/icescape/#hly1101), which detected a massive under-ice bloom with
371 rates of over 10 g C $m^{-2}$ $d^{-1}$ in the Hanna Shoal region in July (72.6324; -168.726; Arrigo et al.,
372 2012). Whether such high growth rates are present at this location every year is unknown, but
373 with thinning ice and a more fractured ice pack before the main marginal ice zone arrives, this
374 phenomenon is expected to be more prevalent. The annual IPP of 173 g C $m^{-2}$ $yr^{-1}$ based on *in*
375 *situ* observations is higher than satellite derived rates of <100 g C $m^{-2}$ $yr^{-1}$ (Arrigo et al., 2008),
376 which may be due to the inability of satellites to detect and account for both under-ice production
377 and the SPM. This suggests that for the northern Chukchi sea under ice and subsurface
378 production contribute approximately 40% to annual PP rates.
379
380 *4.4 Beaufort Shelf*
381 The presence of an SPM on the Beaufort shelf in June indicates that, like in the other
382 regions, PP at the surface has been occurring prior to ice retreat, most likely in May. June
383 observations are clustered close to Barrow Canyon and therefore may not be representative of the
384 entire Beaufort shelf. The highest IPP was observed during June and into July. These high rates
385 have in the past been attributed to the retreating ice edge and upwelling that provides nutrients
386 for phytoplankton growth (Carmack et al., 2004; Mundy et al., 2009). IPP in these regions has
387 been recorded as high as 200 mg C $m^{-2}$ $d^{-1}$ (Carmack et al., 2004) contributing ~ 31 g C $m^{-2}$ over
388 three weeks which is a large fraction of the annual production for this region (Mundy et al.,
389 2009). Hot spots of PP in July were located close to the coast, near the Mackenzie Canyon,
390 which coincided with the presence of warm surface water from the Mackenzie plume that could
391 provide nutrients for phytoplankton growth (Nghiem et al., 2014). IPP in both June and July was
392 approximately half that observed in the Chukchi Sea. Nutrients enter the Beaufort shelf via the

Mackenzie River outflow. However, this also introduces both freshwater, which strengthens stratification, and high turbidity, which limits light penetration (Carmack and MacDonald, 2002; Ardyna et al., 2016). Overall, although the Beaufort shelf is productive in localized spots and has the highest IPP rates of the PAR interior shelves, IPP is low for an Arctic shelf system. The annual estimate of 86 g C $m^{-2}$ $yr^{-1}$ does not include the under-ice production, which could conservatively boost this value to ~ 100 g C $m^{-2}$ $yr^{-1}$. Previous estimates are similar to those seen in this dataset. Satellite values of PP range from ~150 g C $m^{-2}$ $yr^{-1}$ close to the coast to <50 g C $m^{-2}$ $yr^{-1}$ near the shelf break (Arrigo et al., 2008). However, lower rates of 30 – 70 g C $m^{-2}$ $yr^{-1}$ (Sakshaug et al., 2004) and ~ 60 g C $m^{-2}$ $yr^{-1}$ (Ardyna et al. 2013) were estimated from *in situ* observations encompassing the shelf and slope area of the Beaufort Sea.

*4.5 East Siberian Sea*

The East Siberian Sea is chronically under-sampled, and therefore our observations are preliminary. This region has always been considered to be nutrient poor, suggesting that the magnitude of phytoplankton growth is ultimately nutrient limited (Codispoti and Richards, 1968), while the vertical distribution, appears to follow light limited patterns. Our rates of 8 g C $m^{-2}$ $yr^{-1}$ are consistent with other estimates (Codispoti et al., 2013; Popova et al., 2010) that show this part of the Siberian shelf to be the least productive area in the PAR. Although there is no indication of under-ice blooms in this dataset, there is no reason to expect that phytoplankton are not capable of production to the level supported by the available nutrients under the ice in early spring. Annual primary production from nutrient drawn has been estimated at only ~ 8 g C $m^{-2}$ $yr^{-1}$ (Codispoti et al., 2013), although model simulations for an ice-free Arctic suggest that a slightly higher rate of about 29 g C $m^{-2}$ $yr^{-1}$ (Slagstad et al., 2011) is possible, which is comparable to satellite-based estimates of <50 g C $m^{-2}$ $yr^{-1}$ (Arrigo et al., 2008). The low nutrient concentrations in this region are such that even a longer open water season would not make the East Siberian Sea comparable in production to its neighboring Chukchi Sea. Shelf break upwelling or encroachment of Atlantic water from northern sections of the East Siberian and Laptev Seas would be required to boost nutrient availability and hence increase PP rates.

*4.6 Chukchi Plateau and Canada Basin*

PP throughout the euphotic zone in the basin and over the Chukchi Plateau show classic light-limited profiles, with rates highest at the surface. The Basin is an oligotrophic environment in which nitrate concentrations within the euphotic zone are as low as ~ 0 µM even in winter (Codispoti et al., 2013; Varela et al., 2013). IPP remains low throughout the growing season compared to the shelf areas, with highest magnitudes of ~ 400 mg C $m^{-2}$ $d^{-1}$ in June and July, and annual totals of 37 g C $m^{-2}$ $yr^{-1}$. Previous estimates of annual rates have ranged from <15 g C $m^{-2}$ $yr^{-1}$ (Codispoti et al., 2013) based on nutrient drawdown to <50 g C $m^{-2}$ $yr^{-1}$ from satellite retrievals (Arrigo et al., 2008), and chlorophyll-derived PP climatology (Ardyna et al. 2013). Recent high temporal resolution measurements of chlorophyll, made from Ice-Tethered Profilers, show the formation of subsurface chlorophyll maxima during July and August at ~ 50 m with concentrations of ~0.3 µg $L^{-1}$ (Laney et al., 2014), however, it is not known whether this represents an true SPM or a high chlorophyll adaptation to low light conditions. The lack of nutrients does suggest that even with a longer growing season, IPP will still be low. However, changes in circulation, shallowing of the Atlantic water mass layer or the potential impact of atmospheric forcing in the form of storms, tides and waves could erode the vertical stratification providing a source of nutrients to the upper water column (Rainville and Woodgate, 2009; Rainville et al., 2011)

*4.7 Decadal differences*

There is an indication of a shift in both the vertical distribution and magnitude of seasonal IPP on the southern Chukchi shelf in August. The roughly homogenous profile, with a very small SPM around 40 m observed in the 1959 and 1960 data, suggests the presence of a weak nutricline at 40 m. The low overall IPP during this period is also representative of nutrient-limited growth even at the SPM. In comparison, data collected in the 2000s show the highest growth at the surface which perhaps indicates that the nutricline was either too deep for phytoplankton growth or that there was an increase in surface nutrient concentration. Since the 2000s, IPP has also increased significantly, which indicates more available nutrients during August. We propose four possible explanations for the changes in magnitude and distribution of PP. The first is a deepening of the thermocline since the 1960s. The cruise report from the 1959 and 1960 dataset shows stratification with the thermocline at approximately 20 m or shallower (Dawson, 1965). Data from the central Chukchi Sea moorings in 1990 through 1991 (locations

454 shown in Fig 4A) indicate that warming in August extended to approximately 40 m (Woodgate
455 et al., 2005) and that this surface warming has intensified in this region since 2000 (Steele et al.,
456 2008). A deeper thermocline could remove the nutricline from the euphotic zone limiting
457 phytoplankton growth at the surface, eliminating the SPM, and possibly shifting it to later in the
458 season (July), however, it would also reduce IPP. The second explanation involves increased
459 vertical mixing due to expanded open water conditions, which increases the fetch and could be
460 mixing nutrients up to the surface, however, this theory does run counter to the increased thermal
461 stratification theory. Thirdly, although there is no evidence of a change in the distribution of
462 water masses in this region since the early 1960s, observations show fluctuations in the flux of
463 water through the Bering Strait (Woodgate et al., 2006), and increases of up to 50% in the flow
464 volume since 2001, which may enhance nutrient supply to the central southern Chukchi
465 (Woodgate et al., 2015). Northeasterly and easterly winds can reverse the flow along the Alaska
466 coastline perhaps shifting the surface distribution of water masses (Winsor and Chapman, 2004).
467 In fact Bond and Stabeno (this issue) found a great deal of year-to-year variability in flow
468 direction and strength on the Chukchi shelf, particularly in the warm season. Finally,
469 methodological differences could have caused depressed PP measurements in the 1959 and 1960
470 observations relative to present data. Trace metal contamination could have affected PP
471 measurements collected before the 1980s, due to the lack of trace-metal clean sampling
472 procedures, uptake and release of biologically active metals by glass incubation vessels, and
473 trace metal contamination of $^{14}C$ solution stocks. (Fitzwater et al., 1982). Copper contamination,
474 in particular, was linked with depressed PP rates (Fitzwater et al., 1982).
475 Changes on the Hanna Shoal transect between 1993, 2002 and 2004 appear to be linked to
476 the earlier timing of sea-ice retreat. In 1993, a surface phytoplankton bloom was present at the
477 beginning of August under persistent ice cover. However, the magnitude of PP was low, perhaps
478 indicating the very beginning of phytoplankton growth. In 2002 and 2004, open water conditions
479 were present at the beginning of August and the highest PP was at the SPM, suggesting that the
480 surface bloom had already taken place. This proposes a shift in phenology for this area, with the
481 surface bloom now occurring earlier in the season. This argument aligns with our understanding
482 of change in this area, with surface blooms occurring earlier in the year due to thinner ice and
483 quicker ice retreat (Wassmann, 2011). It is possible that this phenomenon has been happening

484 across the entire PAR. However this assumption is difficult to confirm due to the lack of repeat
485 measurements over decadal timescale.
486
487
488
489 **5.0 Conclusion**
490 The Chirikov Basin and Chukchi shelf are the most productive regions of the PAR due to
491 the supply of nutrients from the Bering shelf. These regions are also experiencing the greatest
492 decrease in sea-ice persistence and subsequent solar warming and could be the most impacted in
493 the PAR. The East Siberian Sea, Chukchi Plateau, and Canada Basin are the least productive
494 regions of the PAR, associated with very low nutrient concentrations, even after winter mixing.
495 These regions, which historically experienced very low open water area, are now ice free in
496 August and September increasing the annual light flux. Despite more light availability, the East
497 Siberian Sea, Chukchi Plateau and Canada Basin will remain among the regions with the lowest
498 production in the Arctic, unless there are significant changes in nutrient input.
499 This synthesis shows the widespread occurrence of SPM during May through July across the
500 Chirikov Basin and Chukchi shelf. The presence of the SPM soon after ice retreat points towards
501 the presence of significant under-ice production, which has so far been elusive due to difficulties
502 in making observations early in the year. It is likely that while under-ice blooms have always
503 occurred initiated by melt ponds and leads, the Arctic of the future could see an increase in the
504 productivity of these under-ice blooms and possibly an earlier onset due to thinning ice.
505 Attempts to quantify this early production should be considered critical, due to the impact of
506 changes in plankton phenology on food webs.
507 One pattern that is consistent across the PAR is the near surface PP maximum in the fall,
508 linked with depressed growth rates. Both light and nutrients are limiting factors at this time of
509 year with reduced incident irradiance and depleted nutrients from prior growth. Satellite data has
510 shown that the incidence of fall blooms is increasing in the Arctic due to delayed freeze-up and
511 increased exposure to surface wind stress (Ardyna et al., 2014). The future prevalence of a fall
512 bloom could have significant impacts on consumers who exploit this windfall to increase
513 recruitment and winter survival. Unfortunately many regions have a sparse coverage of

observations during the fall, which severely limits our ability to evaluate IPP during this time compared to the rest of the year.

The lack of consistent repeat observations over decadal timescales makes the identification of long-term changes in the magnitude and distribution of primary production in the PAR unattainable at the current time; although we have been able to identify a few indications of change that point towards shifting phenology in the PAR. Long-term observational programs of primary production in the PAR should be considered a priority for understanding the future impacts of climate change in this region.

**Acknowledgments**

This study is part of the Synthesis of Arctic Research (SOAR) and was funded in part by the U.S. Department of the Interior, Bureau of Ocean Energy Management, Environmental Studies Program through Interagency Agreement No. M11PG00034 with the U.S. Department of Commerce, National Oceanic and Atmospheric Administration (NOAA), Office of Oceanic and Atmospheric Research (OAR), Pacific Marine Environmental Laboratory (PMEL).

Support for Lee was provided by the Korea Research Foundation (KRF) grant funded by the Korea government (MEST; No. 2016015679). Financial support for Varela's research was provided by a Discovery Grant Individual from the Natural Sciences and Engineering Research Council of Canada (Varela only PI) and by the Canadian IPY-C3O Project (E. Carmack. lead PI; Varela, co-PI). This manuscript was improved by the insightful comments of anonymous reviewers and Dr. Paty Matria. Our thanks to Chelsea Wehn, David Ruble and Russel Ives for assistance in database analysis.

## References


Ardyna, M., Babin, M., Devred, E., Forest, A., Gosselin, M., Raimbault, P. and Tremblay, J.-E., 2016. Shelf-basin gradients shape ecological phytoplankton niches and community compositon in the coastal Arctic Ocean (Beaufort Sea). Limnology and Oceanography. in review.

Ardyna, M., Babin, M., Gosselin, M., Devred, E., Belanger, S., Matsuoka, A. and Tremblay, J. E., 2013. Parameterization of vertical chlorophyll a in the Arctic Ocean: impact of the subsurface chlorophyll maximum on regional, seasonal, and annual primary production estimates. Biogeosciences. 10(6), 4383-4404. 10.5194/bg-10-4383-2013.

Ardyna, M., Babin, M., Gosselin, M., Devred, E., Rainville, L. and Tremblay, J. E., 2014. Recent Arctic Ocean sea ice loss triggers novel fall phytoplankton blooms. Geophysical Research Letters. 41(17), 6207-6212. 10.1002/2014GL061047.

Ardyna, M., Gosselin, M., Michel, C., Poulin, M. and Tremblay, J.-E., 2011. Environmental forcing of phytoplankton community structure and function in the Canadian High Arctic: contrasting oligotrophic and eutrophic regions Marine Ecology Progress Series. 442, 37-57.

Arrigo, K. R., Matrai, P. A. and van Dijken, G. L., 2011. Primary productivity in the Arctic Ocean: Impacts of complex optical properties and subsurface chlorophyll maxima on large-scale estimates. Journal of Geophysical Research. 116(C11022), doi:10.1029/2011JC007273.

Arrigo, K. R., Perovich, D. K., Pickart, R. S., Brown, Z. W., Van Dijken, G. L., Lowry, K. E., Mills, M. M., Palmer, M., A, Balch, W. M., Bahr, F., Bates, N. R., Benitez-Nelson, C., Bowler, B., Brownlee, E., Ehn, J. K., Frey, K. E., Garley, R., Laney, S. R., Lubelczyk, L., Mathis, J., Matsuoka, A., Mitchell, B. G., Moore, G. W. K., Ortega-Retuerta, E., Pal, S., Polashenski, C. M., Reynolds, R. A., Schieber, B., Sosik, H. M., Stephens, M. and Swift, J. H., 2012. Massive Phytoplankton Blooms Under Arctic Sea Ice. . Science. 336, 1408.

592 Arrigo, K. R., van Dijken, G. and Pabi, S., 2008. Impact of a shrinking Arctic ice cover on marine
593 primary production. Geophysical Research Letters. 35, L19603. doi:10.1029/2008GL035028.
594 Arrigo, K. R. and van Dijken, G. L., 2011. Secular trends in Arctic Ocean net primary production
595 Journal of Geophysical Research. 116, C09011. doi:10.1029/2011JC007151.
596 Brown, Z. W., Lowry, K. E., Palmer, M. A., van Dijken, G. L., Mills, M. M., Pickart, R. S. and
597 Arrigo, K. R., 2015. Characterizing the subsurface chlorophyll a maximum in the Chukchi Sea
598 and Canada Basin. Deep-Sea Research Part Ii-Topical Studies in Oceanography. 118, 88-104.
599 10.1016/j.dsr2.2015.02.010.
600 Brown, Z. W., van Dijken, G. L. and Arrigo, K. R., 2011. A reassessment of primary production
601 and environmental change in the Bering Sea. Journal of Geophysical Research-Oceans. 116,
602 10.1029/2010jc006766.
603 Brugel, S., Nozais, C., Poulin, M., Tremblay, J. E., Miller, L. A., Simpson, K. G., Gratton, Y. and
604 Demers, S., 2009. Phytoplankton biomass and production in the southeastern Beaufort Sea in
605 autumn 2002 and 2003. Marine Ecology Progress Series. 377, 63-77. 10.3354/meps07808.
606 Carmack, E. C. and MacDonald, R. W., 2002. Oceanography of the Canadian shelf of the Beaufort
607 Sea: A setting for marine life. Arctic. 55, 29-45.
608 Carmack, E. C., Macdonald, R. W. and Jasper, S., 2004. Phytoplankton productivity on the
609 Canadian Shelf of the Beaufort Sea. Marine Ecology Progress Series. 277, 37-50.
610 Cavalieri, D., Parkinson, C., Gloersen, P. and Zwally, H., 1996 updated yearly. Sea Ice
611 Concentrations from Nimbus-7 SMMR and DMSP SSM/I-SSMIS Passive Microwave Data,
612 Version 1. Boulder, Colorado USA, NASA National Snow and Ice Data Center Distributed
613 Active Archive Center.

614 Churnside, J. H. and Marchbanks, R. D., 2015. Subsurface plankton layers in the Arctic Ocean.
615 Geophysical Research Letters. 42(12), 4896-4902. 10.1002/2015GL064503.
616 Coachman, L. K., 1993. On the Flow Field in the Chirikov Basin. Continental Shelf Research.
617 13(5-6), 481-508. Doi 10.1016/0278-4343(93)90092-C.
618 Codispoti, L. A., Kelly, V., Thessen, A., Matrai, P., Suttles, S., Hill, V., Steele, M. and Light, B.,
619 2013. Synthesis of primary production in the Arctic Ocean: III. Nitrate and phosphate based
620 estimates of net community production. Progress in Oceanography. 110, 126-150.
621 10.1016/j.pocean.2012.11.006.
622 Codispoti, L. A. and Richards, F. A., 1968. Micronutrient Distributions in East Siberian and
623 Laptev Seas during Summer 1963. Arctic. 21(2), 67-&.
624 Cooper, L. W., Cota, G. F., Pomeroy, L. R., Grebmeier, J. M. and Whitledge, T. E., 1999.
625 Modification of NO, PO and NO/PO during flow across the Bering and Chukchi shelves:
626 Implications for use as Arctic water mass tracers. Journal of Geophysical Research. 104(C4),
627 7827-7235.
628 Cullen, J. J., 1982. The Deep Chlorophyll Maximum - Comparing Vertical Profiles of
629 Chlorophyll-A. Canadian Journal of Fisheries and Aquatic Sciences. 39(5), 791-803. Doi
630 10.1139/F82-108.
631 Dawson, W. A., 1965. Phytoplankton Data from the Chukchi Sea, University of Washington,
632 Department of Oceanography. Technical Report No. 117
633 Fitzwater, S. E., Knauer, G. A. and Martin, J. H., 1982. Metal contamination and its effect on
634 primary production measurements primary production
635 C14. Limnology and Oceanography. 27(3), 544-551.

636 Frey, K. E., Maslanik, J., Kinney, J. C. and Maslowski, W., 2014. Recent Variability in Sea Ice
637 Cover, Age, and Thickness in the Pacific Arctic Region. In: J. M. Grebmeier and W.
638 Maslowski (Eds.), The Pacific Arctic Region.Springer, Place, Published,31-63.
639 Frey, K. E., Moore, G. W. K., Cooper, L. W. and Grebmeier, J. M., 2015. Divergent patterns of
640 recent sea ice cover across the Bering, Chukchi, and Beaufort seas of the Pacific Arctic Region.
641 Progress in Oceanography. 136, 32-49. 10.1016/j.pocean.2015.05.009.
642 Gong, D. L. and Pickart, R. S., 2015. Summertime circulation in the eastern Chukchi Sea. Deep-
643 Sea Research Part Ii-Topical Studies in Oceanography. 118, 18-31. 10.1016/j.dsr2.2015.02.006.
644 Grebmeier, J. M., McRoy, C. P. and Feder, H. M., 1988. Pelagic-benthic coupling on the shelf of
645 the northern Bering and Chukchi Seas. I. Food supply source and benthic biomass. . Marine
646 Ecology Progress Series. 48.
647 Hill, V. and Cota, G., 2005. Spatial patterns of primary production on the shelf, slope and basin of
648 the Western Arctic in 2002. Deep-Sea Research Part Ii-Topical Studies in Oceanography.
649 52(24-26), 3344-3354. 10.1016/j.dsr2.2005.10.001.
650 Hill, V. J., Matrai, P. A., Olson, E., Suttles, S., Steele, M., Codispoti, L. A. and Zimmerman, R.
651 C., 2013. Synthesis of integrated primary production in the Arctic Ocean: II. In situ and
652 remotely sensed estimates. Progress in Oceanography. 110, 107-125.
653 10.1016/j.pocean.2012.11.005.
654 Kahru, M., Lee, Z., Mitchell, B. G. and Nevison, C. D., 2016. Effects of sea ice cover on satellite-
655 detected primary production in the Arctic Ocean. Global Change Biology. 12(20160233),
656 http://dx.doi.org/10.1098/rsbl.2016.0223.
657 Kwok, R. and Rothrock, D. A., 2009. Decline in Arctic sea ice thickness from submarine and
658 ICESat records: 1958-2008. Geophysical Research Letters. 36, 10.1029/2009gl039035.

659 Laney, S. R., Krishfield, R. A., Toole, J. M., Hammar, T. R., Ashjian, C. J. and Timmermans, M.
660 L., 2014. Assessing algal biomass and bio-optical distributions in perennially ice-covered polar
661 ocean ecosystems. Polar Science. 8(2), 73-85. 10.1016/j.polar.2013.12.003.
662 Lee, S. H., Stockwell, D. and Whitledge, T. E., 2010. Uptake rates of dissolved inorganic carbon
663 and nitrogen by under-ice phytoplankton in the Canada Basin in summer 2005. Polar Biology.
664 33(8), 1027-1036. 10.1007/s00300-010-0781-4.
665 Lee, S. H. and Whitledge, T. E., 2005. Primary and new production in the deep Canada Basin
666 during summer 2002 Polar Biology. 28, 190-197.
667 Leu, E., Soreide, J. E., Hessen, D. O., Falk-Peterson, S. and Berge, J., 2011. Consequences of
668 changing sea-ice cover for primary and secondary producers in the European Arctic shelf seas:
669 Timing, quantity, and quality. Progress in Oceanography. 90, 18-32.
670 Lowry, K. E., van Dijken, G. L. and Arrigo, K. R., 2014. Evidence of under-ice phytoplankton
671 blooms in the Chukchi Sea from 1998 to 2012. Deep-Sea Research Part Ii-Topical Studies in
672 Oceanography. 105, 105-117. 10.1016/j.dsr2.2014.03.013.
673 Martin, J., Tremblay, J.-E., Gagnon, J., Tremblay, G., Lapoussiere, A., Jose, C., Poulin, M.,
674 Gosselin, M., Gratton, Y. and Michel, C., 2010. Prevalence, structure and properties of
675 subsurface chlorophyll maxima in Canadian Arctic waters Canadian Arctic. Marine Ecology
676 Progress Series. 42, 69-84. doi: 10.3354/meps08666.
677 Martin, J. H., Dumont, D. and Tremblay, J., 2013. Contribution of subsurface chlorophyll maxima
678 to primary production in the coastal Beaufort Sea (Canadian Arctic): A model assessment.
679 Journal of Geophysical Research. DOI 10.1002/2013JC008843.

680 Martini, K. I. P., Stabeno, P. J., Ladd, C., Winsor, P., Weingartner, T., Mordy, C. W. and Eisner,
681 L. B., 2016. Dependence of subsurface chlorophyll on seasonal water masses in the Chukchi
682 Sea. Journal of Geophysical Research. 121, doi:10.1002/2015JC011359.
683 Mathis, J., Grebmeier, J. M., Hansell, D. A., Hopcroft, R. R., Kirchman, D. L., Lee, S. H., Moran,
684 S. B., Bates, N., VanLaningham, S., Cross, J. N. and Cai, W.-J., 2014. Carbon Biogeochemistry
685 of the Western Arctic: Primary Production, Carbon Export and the Controls on Ocean
686 Acidification. In: J. M. Grebmeier and W. Maslowski (Eds.), The Pacific Arctic Region:
687 Ecosysten Status and Trends in a Rapidly Changing Environment.Springer Science+Business
688 Media, Place,
689 McLaughlin, F. A. and Carmack, E. C., 2010. Deepening of the nutricline and chlorophyll
690 maximum in the Canada Basin interior, 2003-2009. Geophysical Research Letters. 37,
691 10.1029/2010gl045459.
692 Monier, A., Comte, J., Babin, M., Forest, A., Matsuoka, A. and Lovejoy, C., 2015. Oceanographic
693 structure drives the assembly processes of microbial eukaryotic communities. Isme Journal.
694 9(4), 990-1002. 10.1038/ismej.2014.197.
695 Mundy, C. J., Gosselin, M., Ehn, J. K., Gratton, Y., Rossnagel, A., Barber, D., Martin, J.,
696 Tremblay, J.-E., Palmer, M., Arrigo, K. R., Darnis, G., Fortier, L., Else, B. and Papakyriakou,
697 T. N., 2009. Contribution of under-ice primary production to an ice-edge upwelling
698 phytoplankton bloom in the Canadian Beaufort Sea. Geophysical Research Letters. 36, L17601.
699 doi:10.1029/2009GL038837.
700 Nghiem, S. V., Hall, D. K., Rigor, I. G., Li, P. and Neumann, G., 2014. Effects of Mackenzie
701 River discharge and bathymetry on sea ice in the Beaufort Sea. Geophysical Research Letters.
702 41(3), 873-879. 10.1002/2013GL058956.

703 Peralta-Ferriz, C. and Woodgate, R. A., 2015. Seasonal and interannual variability of pan-Arctic
704 surface mixed layer properties from 1979 to 2012 from hydrographic data, and the dominance
705 of stratification for multiyear mixed layer depth shoaling. Progress in Oceanography. 134, 19-
706 53. 10.1016/j.pocean.2014.12.005.
707 Perovich, D. K., Richter-Menge, J. A., Jones, K. F. and Light, B., 2008. Sunlight, water, and ice:
708 Extreme Arctic sea ice melt during the summer of 2007. . Geophysical Research Letters. 35.
709 Popova, E. E., Yool, A., Coward, A. C., Aksenov, Y. K., Alderson, S. G., de Cuevas, B. A. and
710 Anderson, T. R., 2010. Control of primary production in the Arctic by nutrients and light:
711 insights from a high resolution ocean general circulation model Biogeosciences. 7, 3569-3591.
712 doi:10.5194/bg-7-3569-2010.
713 Rainville, L., Lee, C. M. and Woodgate, R. A., 2011. Impact of Wind-Driven Mixing in the Arctic
714 Ocean. Oceanography. 24(3), 136-145.
715 Rainville, L. and Woodgate, R. A., 2009. Observations of internal wave generation in the
716 seasonally ice-free Arctic. Geophysical Research Letters. 36, Artn L23604
717 10.1029/2009gl041291.
718 Sakshaug, E., Stein, R. and Macdonald, R. W., 2004. Primary and Secondary Production in the
719 Arctic Seas. In: R. Stein and R. W. Macdonald (Eds.), The Organic Carbon Cycle in the Arctic
720 Ocean.Springer, Place, Published,57-82.
721 Sharples, J., Moore, C. M., Rippeth, T. P., Holligan, P. M., Hydes, D. J., Fisher, N. R. and
722 Simpson, J. H., 2001. Phytoplankton distribution and survival in the thermocline. Limnology
723 and Oceanography. 46(3), 486-496.

724 Slagstad, D., Ellingsen, I. H. and Wassmann, P., 2011. Evaluating primary and secondary
725 production in an Arctic Ocean void of summer sea ice: An experimental simulation approach.
726 Progress in Oceanography. 90, 117-131.
727 Soreide, J. E., Leu, E., Berge, J., Graeve, M. and Falk-Petersen, S., 2010. Timing of blooms, algal
728 food quality and Calanus glacialis reproduction and growth in a changing Arctic. Global
729 Change Biology. 16(11), 3154-3163. 10.1111/j.1365-2486.2010.02175.x.
730 Spall, M. A., Pickart, R. S., Brugler, E. T., Moore, G. W. K., Thomas, L. and Arrigo, K. R., 2014.
731 Role of shelfbreak upwelling in the formation of a massive under-ice bloom in the Chukchi
732 Sea. Deep-Sea Research Part Ii-Topical Studies in Oceanography. 105, 17-29.
733 10.1016/j.dsr2.2014.03.017.
734 Springer, A. M. and McRoy, C. P., 1993. The paradox of pelagic food webs in the northern Bering
735 Sea-III.Patterns of primary productivity Continental Shelf Research. 13(5/6), 575-599.
736 Springer, A. M., McRoy, C. P. and Flint, M. V., 1996. The Bering Sea Green Belt: Shelf-edge
737 processes and ecosystem production. Fisheries Oceanography. 5(3-4), 205-223. DOI
738 10.1111/j.1365-2419.1996.tb00118.x.
739 Steele, M., Ermold, W. and Zhang, J. 2008 Arctic Ocean surface warming trends over the past 100
740 years. Geophysical Research Letters 35, DOI: doi:10.1029/2007GL031651
741 Stringer, W. J. and Groves, J. E., 1991. Location and Areal Extent of Polynyas in the Bering and
742 Chukchi Seas. Arctic. 44, 164-171.
743 Timmermans, M.-L. and Proshutinsky, A., 2015. The Arctic: Sea surface temperature, in State of
744 the Climate 2014. Bulletin of the American Meteorological Society. 96(7), S147-148.

745 Varela, D. E., Crawford, D. W., Wrohan, I. A., Wyatt, S. N. and Carmack, E. C., 2013. Pelagic
746 primary productivity and upper ocean nutrient dynamics across Subarctic and Arctic Seas.
747 Journal of Geophysical Research-Oceans. 118(12), 7132-7152. 10.1002/2013JC009211.
748 Wassmann, P., 2011. Arctic marine ecosystems in an era of rapid climate change. Progress in
749 Oceanography. 90(1-4), 1-17. 10.1016/j.pocean.2011.02.002.
750 Winsor, P. and Chapman, D. C., 2004. Pathways of Pacific Water across the Chukchi Sea: A
751 numerical model study. Journal of Geophysical Research-Oceans. 109(C3),
752 10.1029/2003jc001962.
753 Woodgate, R. A., Aagaard, K. and Weingartner, T. R., 2005. A year in the physical oceanography
754 of the Chukchi Sea: Moored measurements from autumn 1990-1991. Deep Sea Research II. 52,
755 3116-3149.
756 Woodgate, R. A., Aagaard, K. and Weingartner, T. R., 2006. Interannual changes in the Bering
757 Strait fluxes of volume, heat and freshwater between 1991 and 2004 Geophysical Research
758 Letters. 33, doi:10.1029/2006GL026931.
759 Woodgate, R. A., Stafford, K. M. and Prahl, F. G., 2015. A Synthesis of Year-Round
760 Interdisciplinary Mooring Measurements in the Bering Strait (1990-2014) and the RUSALCA
761 Years (2004-2011). Oceanography. 28(3), 46-67. 10.5670/oceanog.2015.57.
762
763
764
765
766
767

768 Table 1. Databases, projects and/or cruises included in the analysis for the period 1950 to 2012
769 for the following regions: Chirikov Basin (CB), southern Chukchi (SC), northern Chukchi (NC),
770 Beaufort shelf (BS), East Siberian Sea (ESS), the Chukchi Plateau and Canada Basin (CPCB). N
771 represents the number of stations from each cruise. $^{14}C$ and $^{13}C$ methods refer to the enrichment
772 of water samples with $^{14}C$ or $^{13}C$ bicarbonate solution before incubation.

773

774

| **Database/Cruise** | **Year** | **N** | **Functional regions** | **Measurement methods** |
|---|---|---|---|---|
| ARCSS-PP (http://www.nodc.noaa.gov/ | 1950 to 2007 | 319 | CB,SC,NC,BS,CPCB | $^{14}C$, $^{13}C$, $O_2$. |
| Icescape | 2010, 2011 | 27,23 | CB, SC,NC,BS | $^{14}C$ |
| Rusalca | 2004, 2009, 2012 | 10,21,11 | SC, EES, CPCB | $^{13}C$ |
| ArcticNet (Ardyna et al., 2011) | 2005, 2006, 2011 | 2,1,1 | BS, CPCB | $^{14}C$ |
| CFL (Mundy et al., 2009) | 2008 | 2 | CPCB | $^{14}C$ |
| CASES (Brugel et al., 2009) | 2003, 2004 | 4,6 | BS,CPCB | $^{14}C$ |
| Canada 3 Oceans (Varela et al., 2013) | 2007,2008 | 9,24 | CB,SC,BS, CPCB | $^{13}C$ |
| Healy-2007 | 2007 | 26 | CB | $^{13}C$ |
| Oshoro-Maru | 2007 | 8 | SC | $^{13}C$ |
| XueLong-2008 | 2008 | 22 | BS, CPCB | $^{13}C$ |
| Araon-2010 | 2010 | 118 | EES | $^{13}C$ |

775

776

777

778

779

780

781

782

783

784

785

786

787 Table 2. The average percentage of total integrated primary production (IPP) that occurred
788 between light levels (LL) in each region and season. Numbers in parenthesis are the standard
789 deviation.

| Region LL (%) | May and June (spring) | Total IPP (%) July (early summer) | August (late summer) | September and October (fall) |
|---|---|---|---|---|
| **Chirikov Basin** | | | | |
| **100 – 50%** | 47 (±14) | 49 (±16) | 62 (±9) | 60 (±9) |
| **50 – 30 %** | 21 (±6) | 24 (±6) | 23 (±5) | 22 (±1) |
| **30 – 10%** | 23 (±13) | 24 (±13) | 14 (±7) | 16 (±7) |
| **10 – 1%** | 7 (±8) | 3 (±4) | 1 (±1) | 2 (±2) |
| **Southern Chukchi** | | | | |
| **100 – 50%** | 47 (±13) | 47 (±16) | 68 (±9) | 61 (±8) |
| **50 – 30 %** | 22 (±4) | 26 (±8) | 19 (±3) | 22 (±2) |
| **30 – 10%** | 25 (±8) | 24 (±12) | 12 (±7) | 15 (±6) |
| **10 – 1%** | 6 (±2) | 4 (±5) | 2 (±2) | 2 (±2) |
| **Northern Chukchi** | | | | |
| **100 – 50%** | 46 (±7) | 27 (±21) | 51 (±14) | 64 (±5) |
| **50 – 30 %** | 26 (±4) | 16 (±8) | 19 (±5) | 21 (±3) |
| **30 – 10%** | 23 (±5) | 32 (±13) | 19 (±6) | 13 (±3) |
| **10 – 1%** | 5 (±4) | 25 (±24) | 12 (±14) | 2 (±2) |
| **Beaufort shelf** | | | | |
| **100 – 50%** | 39 (±14) | 49 (±16) | 51 (±11) | 65 (±4) |
| **50 – 30 %** | 25 (±7) | 17 (±5) | 21 (±2) | 20 (±2) |
| **30 – 10%** | 25 (±9) | 23 (±9) | 18 (±7) | 14 (±2) |
| **10 – 1%** | 12 (±12) | 11 (±11) | 4 (±4) | 2 (±1) |
| **East Siberian Sea** | | | | |
| **100 – 50%** | | 67 (±12) | 65 (±16) | 56 (±11) |
| **50 – 30 %** | | 14 (±7) | 14 (±5) | 22 (±4) |
| **30 – 10%** | | 12 (±7) | 12 (±7) | 20 (±12) |
| **10 – 1%** | | 9 (±11) | 9 (±12) | 2 (±2) |
| **Plateau and Basin** | | | | |
| **100 – 50%** | | | 51 (±10) | 61 (±6) |
| **50 – 30 %** | | | 20 (±3) | 21 (±2) |
| **30 – 10%** | | | 21 (±6) | 16 (±5) |
| **10 – 1%** | | | 8 (±6) | 1 (±1) |

790

791

Table 3. Mean daily water column integrated primary production rates (mg C $m^{-2}$ $d^{-1}$) for each month and region. Standard error included in parenthesis. Significant differences between months within the same region are indicated by letters, capitalized letter indicates the highest month, while lower case letters are the significantly lower months. ANOVA 1- way with Tukey's honestly significant difference criterion were used for individual comparisons. NA: No data available. For the southern Chukchi in May, only 2 observations were available, in addition to the mean, the IPP of both stations is also displayed (in square brackets). The number of stations included in monthly estimates are denoted by ns.

| **Region** | **Water column IPP (mg C $m^{-2}$ $d^{-1}$)** | | | | | **Annual IPP (g C $m^{-2}$)** |
|---|---|---|---|---|---|---|
| | **May** | **June** | **July** | **Aug** | **Sept** | |
| **Chirikov Basin** | 1320 (±273) ns 14 | 714 (±235) ns 21 | 1800 (±260) ns 68 | 1655 (±425) ns 35 | 978 (±461) ns 3 | 199 |
| **southern Chukchi** | 2166 (±2014) [152 & 4180] ns 2 | 882 (±245)a ns 10 | 3015 (±840)A ns 22 | 247 (±56)a ns 66 | 437 (±100)a ns 18 | 208 |
| **northern Chukchi** | 407 (±176)a ns 13 | 2401 (±934)B ns 9 | 2016 (±465)A ns 33 | 696 (±110)ab ns 55 | 126 (±22) ns 5 | 173 |
| **Beaufort shelf** | ND | 1427 (±404)A ns 13 | 1004 (±360) ns 18 | 314 (±53) ns 14 | 64 (±18)a v 11 | 86 |
| **East Siberian Sea** | NA | NA | 33 (±15) ns 3 | 93 (±49) ns 8 | 132 (±44) ns 12 | 8 |
| **Chukchi Plateau and Canada Basin** | 90 (±22) ns 4 | 412 (±215) ns 5 | 401 (±124) ns 13 | 240 (±82) ns 31 | 72 (±25) ns 5 | 37 |
| **Monthly g C $m^{-2}$** | 123 | 175 | 256 | 101 | 54 | 710 |

Fig. Legends

Fig. 1. Map of the Pacific Arctic Region (PAR) with functional regions highlighted in different colors and all stations mapped (black dots). Saint Lawrence Island in the Chirikov Basin and Hanna Shoal in the northern Chukchi and Canada Basin regions are identified. Bathymetry taken from IBCAO version 2.

Fig. 2. Seasonal and decadal distribution of sampling stations, A) May and June, B) July, C) August, D) September and October. Regions identified in Fig. 1 are also highlighted. Bathymetry taken from IBCAO version 2.

Fig. 3. Regional and seasonal mean primary production profiles normalized to maximum PP within each profile. Only the 340 stations that included information on the corresponding light levels of the sampling depths are used in this analysis. Each average profile is labeled with the number of profiles (ns) included in the analysis. May and June represent the spring, July the early summer, August the late summer and Sep & Oct the fall.

Fig. 4. A) Map of stations used in the decadal analysis of August vertical profiles for 1959 and 1960, and 2004 to 2007 in the southern Chukchi Sea. Also shown are mooring locations from Woodgate et al., 2005, and major water mass flow over the shelf. B) Mean PP profiles in which PP was normalized to maximum values in each vertical profile. C) Integrated primary production for each decade, with standard error bars and number of profiles (n) included in the analysis. * indicates significant differences between decades, using 1-way ANOVA and Tukey's honestly significant difference criterion for individual comparisons.

Fig. 5. Primary production contours for Hanna Shoal transect occupied from (A) 1 - 4 August of 1993, (B) 6 - 12 August 2002, and (C) 10 - 17 August 2004. Stations along the transect were sampled from shallow to deep.

Fig. 6. Sea-ice concentration for the duration of the Hanna Shoal transect occupation. Sea ice maps are presented for the 1st of August in each year, and the first and last day of primary production measurements. Refer to Fig. 1 for location of Hanna Shoal in wider context of PAR. Sea-ice concentration from Cavalieri et al. (1996 updated yearly). Transect stations are represented as yellow dots, land is represented by green polgons.

Fig. 7. Seasonal distribution of integrated primary production (IPP) at individual stations (circles), and as an interpolated raster. A) May and June, B) July, C) August, D) September and October.

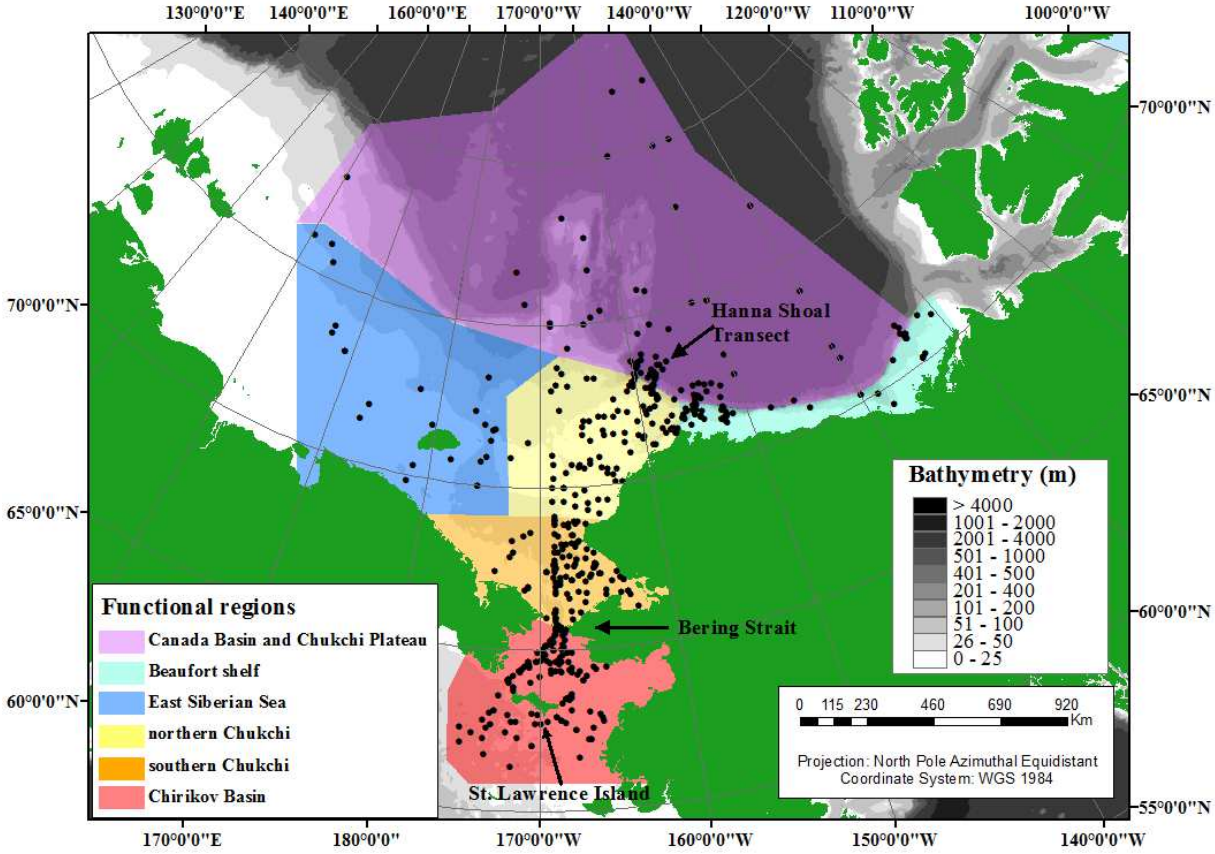
130°0'0"E
140°0'0"E
160°0'0"E
170°0'0"W
140°0'0"W
120°0'0"W
110°0'0"W
100°0'0"W
70°0'0"N
65°0'0"N
60°0'0"N
55°0'0"N
Hanna Shoal
Transect
Bering Strait
St. Lawrence Island
Functional regions
Canada Basin and Chukchi Plateau
Beaufort shelf
East Siberian Sea
northern Chukchi
southern Chukchi
Chirikov Basin
Bathymetry (m)
> 4000
1001 - 2000
2001 - 4000
501 - 1000
401 - 500
201 - 400
101 - 200
51 - 100
26 - 50
0 - 25
0 115 230 460 690 920
Km
Projection: North Pole Azimuthal Equidistant
Coordinate System: WGS 1984
170°0'0"E
180°0'0"
170°0'0"W
160°0'0"W
150°0'0"W
140°0'0"W

Fig. 1

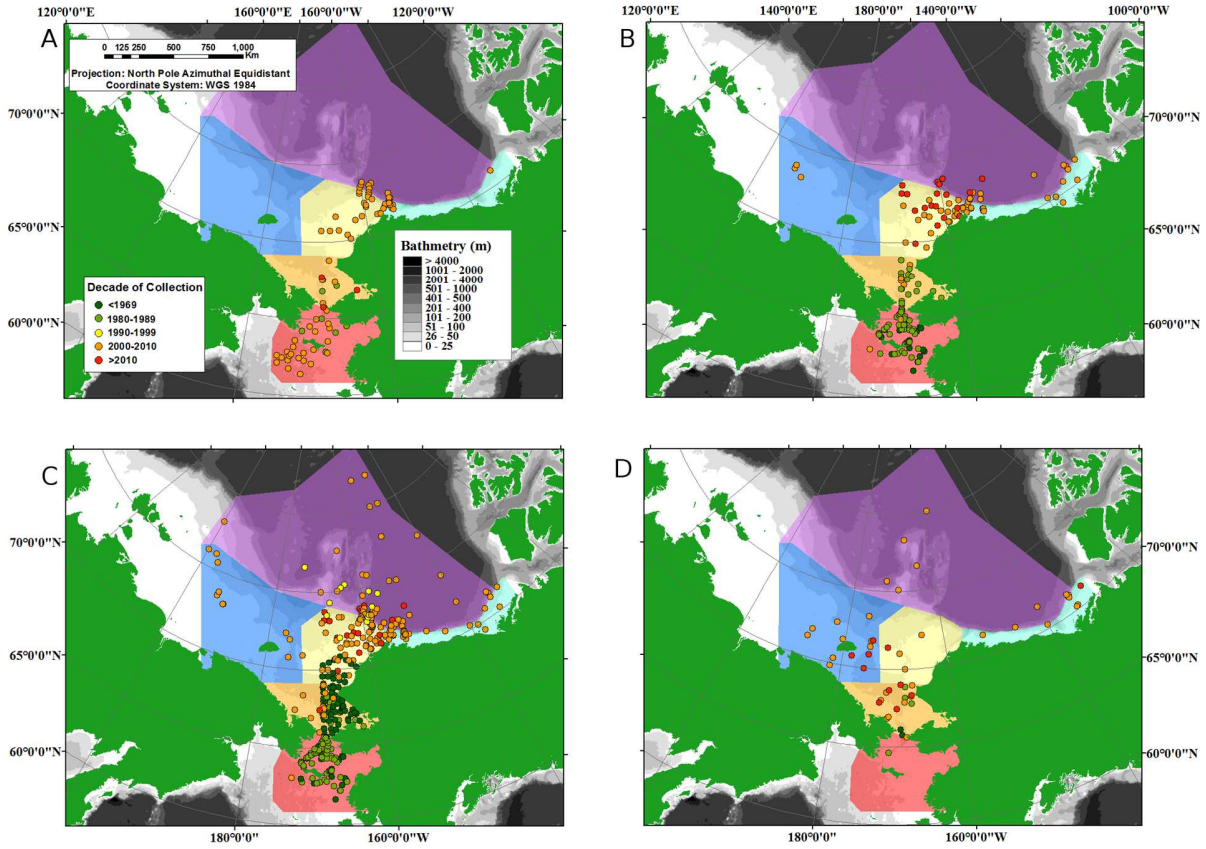
A
B
C
D
120°0'0"E
160°0'0"E
160°0'0"W
120°0'0"W
140°0'0"E
180°0'0"
140°0'0"W
100°0'0"W
70°0'0"N
65°0'0"N
60°0'0"N
180°0'0"
160°0'0"W
0 125 250 500 750 1,000 Km
Projection: North Pole Azimuthal Equidistant
Coordinate System: WGS 1984
Decade of Collection
<1969
1980-1989
1990-1999
2000-2010
>2010
Bathmetry (m)
> 4000
1001 - 2000
2001 - 4000
501 - 1000
401 - 500
201 - 400
101 - 200
51 - 100
26 - 50
0 - 25

Fig. 2

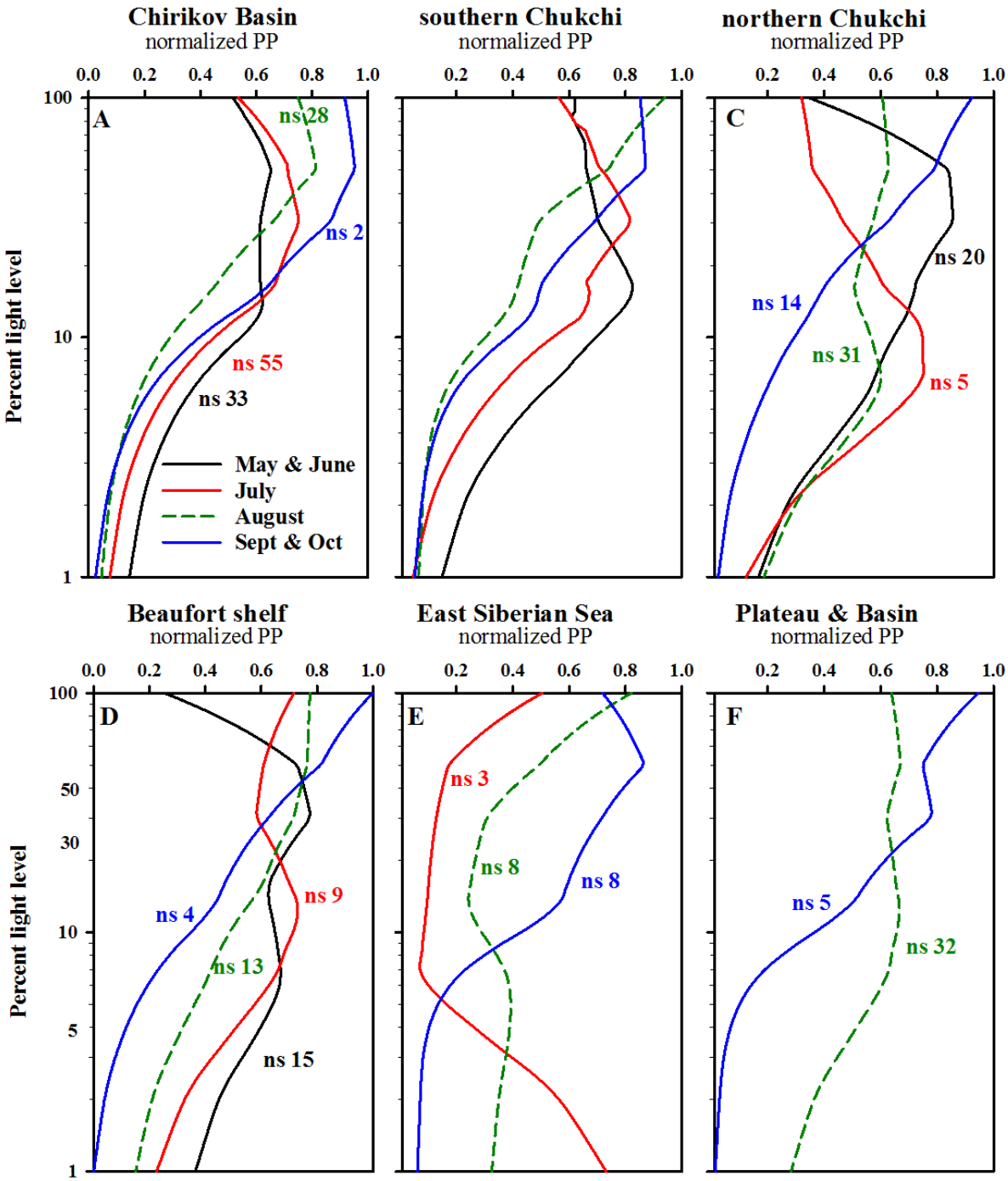


867

868 Fig. 3

869

870

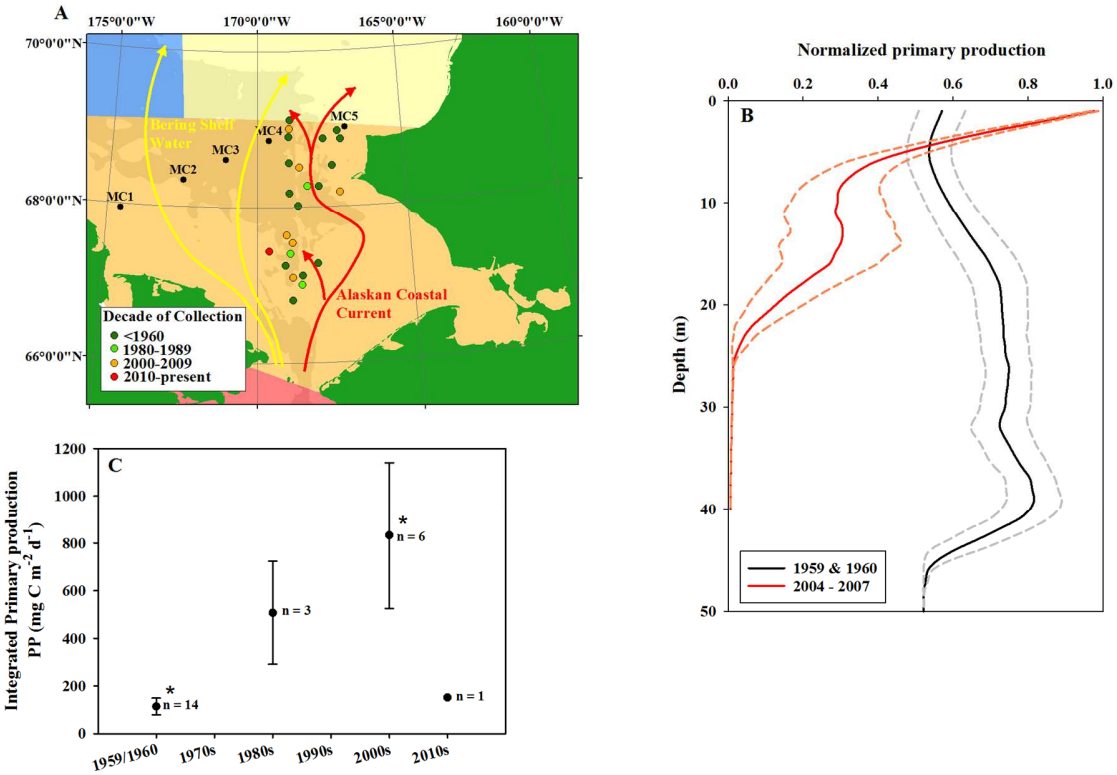
A
175°0'0"W
170°0'0"W
165°0'0"W
160°0'0"W
70°0'0"N
68°0'0"N
66°0'0"N
Bering Shelf Water
MC1
MC2
MC3
MC4
MC5
Alaskan Coastal Current
Decade of Collection
<1960
1980-1989
2000-2009
2010-present
B
Normalized primary production
0.0
0.2
0.4
0.6
0.8
1.0
Depth (m)
0
10
20
30
40
50
1959 & 1960
2004 - 2007
C
Integrated Primary production
PP (mg C m-2 d-1)
1200
1000
800
600
400
200
0
n = 14
n = 3
n = 6
n = 1
1959/1960
1970s
1980s
1990s
2000s
2010s

Fig. 4

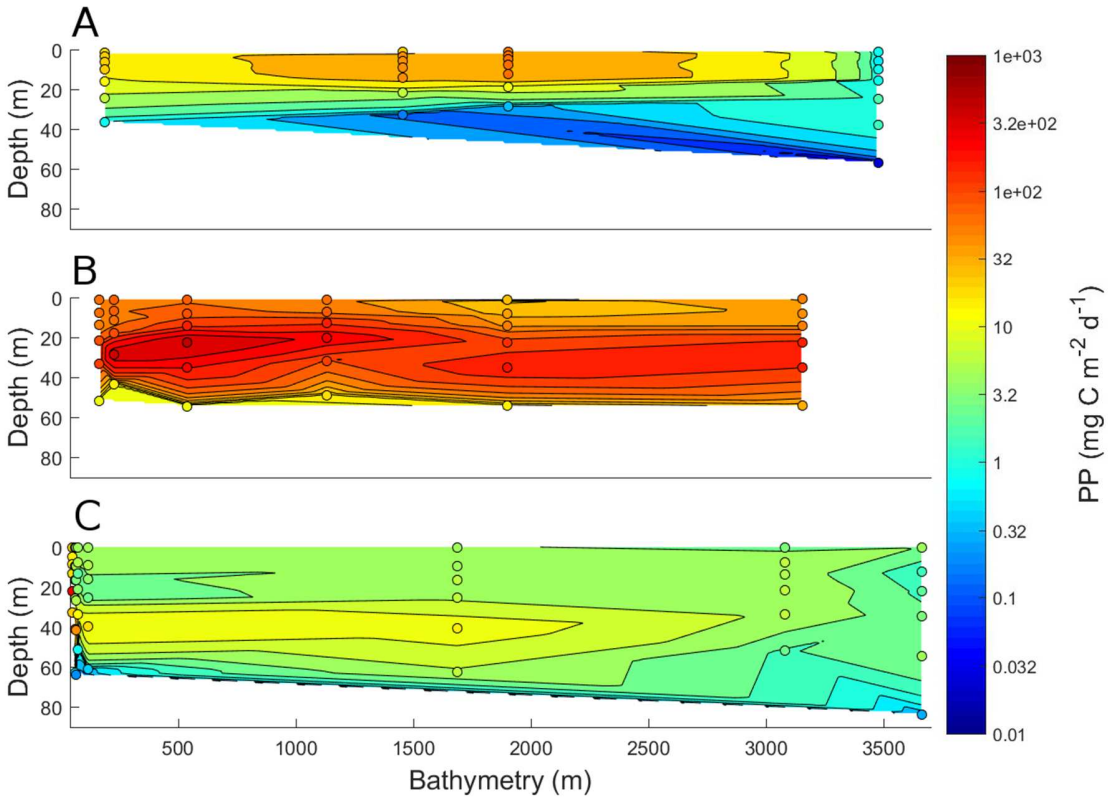
A
B
C
Depth (m)
0
20
40
60
80
500
1000
1500
2000
2500
3000
3500
Bathymetry (m)
1e+03
3.2e+02
1e+02
32
10
3.2
1
0.32
0.1
0.032
0.01
PP (mg C m-2 d-1)

Fig. 5

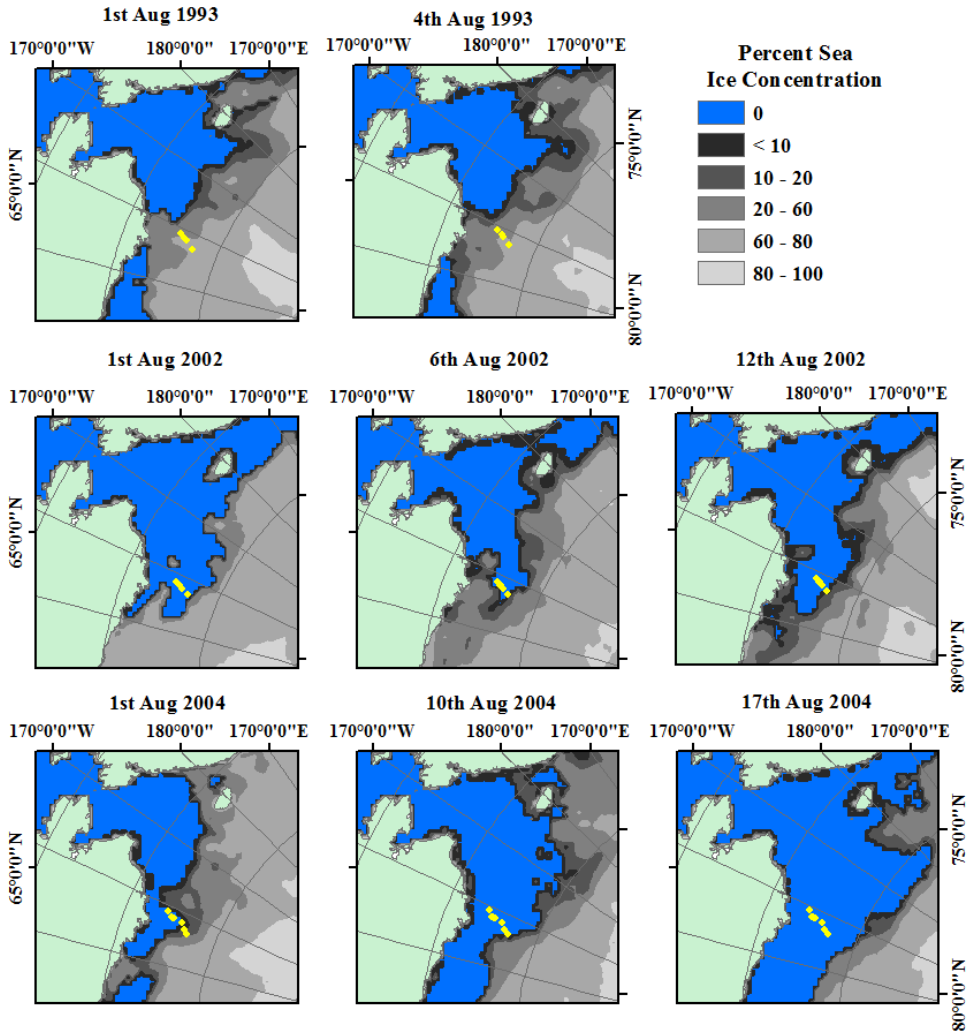


893

894

895 Fig. 6

896

897

898

899

900

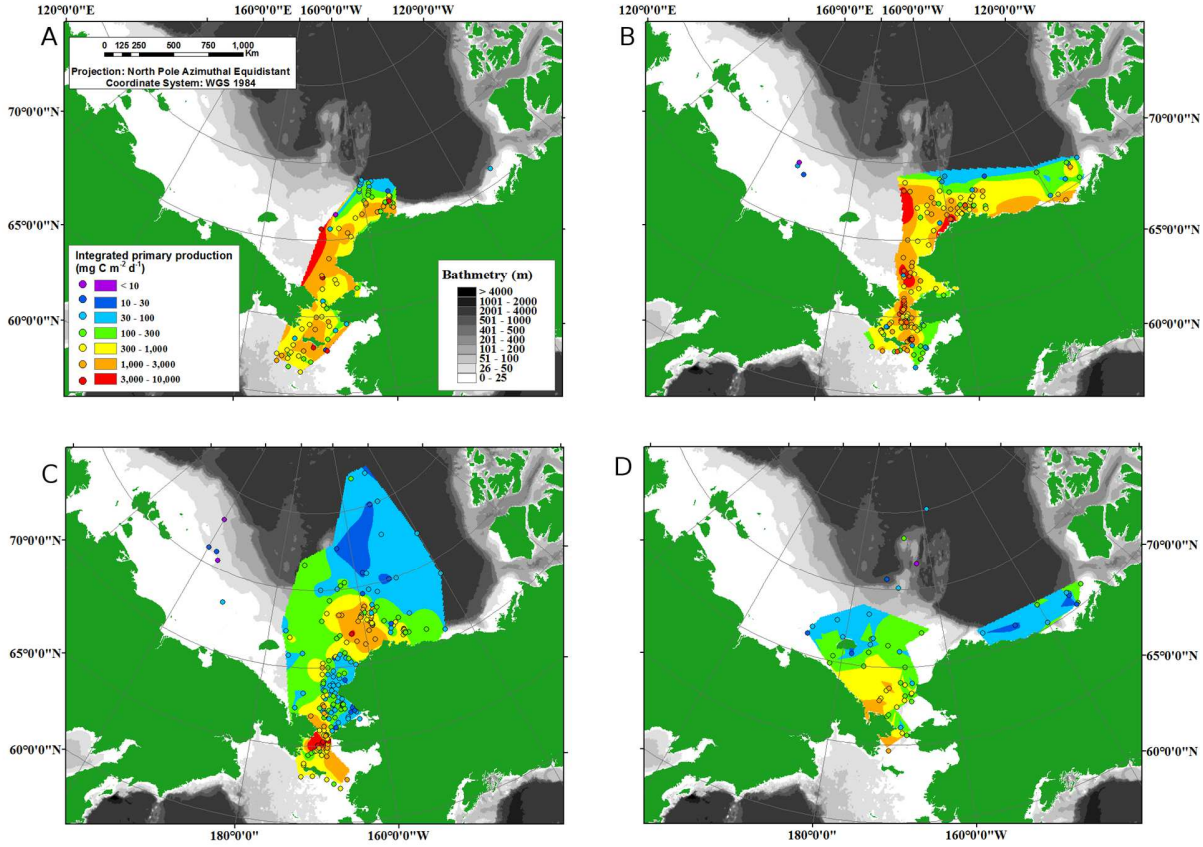
A
B
C
D
120°0'0"E
160°0'0"E
160°0'0"W
120°0'0"W
70°0'0"N
65°0'0"N
60°0'0"N
180°0'0"
0 125 250 500 750 1,000 Km
Projection: North Pole Azimuthal Equidistant
Coordinate System: WGS 1984
Integrated primary production
(mg C m-2 d-1)
< 10
10 - 30
30 - 100
100 - 300
300 - 1,000
1,000 - 3,000
3,000 - 10,000
Bathmetry (m)
> 4000
1001 - 2000
2001 - 4000
501 - 1000
401 - 500
201 - 400
101 - 200
51 - 100
26 - 50
0 - 25

Fig. 7